Journal of Engineering Science and Technology
Vol. 10, No. 4 (2015) 533 - 551

OPTIMAL LOAD SHEDDING BASED ON LINE VOLTAGE STABILITY INDEX USING HARMONY SEARCH ALGORITHM

R. MAGESHVARAN*, T. JAYABARATHI

School of Electrical Engineering, VIT University Vellore - 632014, Tamilnadu, India
*Corresponding Author: rmageshvaran@vit.ac.in

Abstract

Modern power systems have been operated close to their limits for reasons of economic viability. Consequently, a small increase in the load may lead to the Maximum Loading Point (MLP) of the system resulting in voltage collapse. Under such circumstances, the buses for load-shed have been selected based on line voltage stability index and its sensitivities at the operating point. This avoids voltage collapse and improves the system stability. Computational algorithms for minimum load-shed have been developed using the heuristic technique, Harmony search (HS) algorithm. The algorithm proposed in the present paper is implemented on the standard IEEE 14-bus and 25-bus test systems to obtain the optimal load shedding at the selected buses when the systems are operated at their MLP. The effectiveness and efficiency of the proposed method are established by improvements in the line voltage stability index and the bus voltages.

Keywords: Optimal load-shed, Voltage stability, Line voltage stability index, Optimization, Harmony search algorithm.

1. Introduction

Electrical energy is regarded as indispensable to the growth of any country's economy. The main objective of any power generation and distribution utility is to satisfy the energy demand of a customer with a high quality product and uninterrupted service requirements. The continuous increase in the load demand on the power system may lead the system to its voltage collapse point due to which there is a possibility of system blackout. Under such circumstances load shedding is considered as the last line of defence to regain state of operating equilibrium of the power system. Basically there are two strategies of load shedding. The first is based on voltage which is called under voltage load shedding

Nomenclatures

A	*'A'* Constant of transmission line
k, m	The buses to which i^{th} line is connected
L_i	Line voltage stability index
LS_i	Amount of real power load shed at i^{th} bus.
L_{ith}	Threshold value of the line voltage stability index
N_B	Total number of buses
N_G	Total number of generator buses
NLS	Set of buses selected for load shedding
P_k	Sending end real power
P_m	Receiving end real power
S_k	Sending end complex power
S_m	Receiving end complex power
V_k, V_m	The bus voltage magnitude

Greek Symbols

α	The phase angle of *'A'* constant
δ	$\delta_k - \delta_m$ is phase angle across transmission line

Abbreviations

ABC	Artificial bee colony
HS	Harmony search
MLP	Maximum loading point
SFLA	Shuffled frog leaping algorithm

and the other one is based on frequency known as under frequency load shedding. The main objective of load shedding is to provide smooth load relief, in situations where the power system would otherwise go unstable [1].The buses for load shedding are selected based on line voltage stability index and its sensitivities at operating point and the computational algorithm for optimal load shedding was developed using conventional PSO, coordinated aggregation based PSO [2].The under voltage criterion has poor discriminative ability and a proper discrimination for load shed is obtained from the voltage stability margin view point [3]. In [4] a load shedding strategy based on nonlinear programming has been developed in order to maximize the reactive power security.

A statistical approximation procedure to model the distance from point of collapse is introduced in [5] for both preventive and corrective modes. The preventive model takes into account multiple contingencies. The corrective model is based on linear programming for fast calculation of controls in real-time to correct for voltage instability due to specific contingency condition. In [6] a new line voltage stability index, which is reliable and computationally efficient, has been implemented for predicting the voltage collapse of an integrated power system. The index is based on singularity of load flow Jacobian of a transmission line.

According to [7] the minimum Eigen value of load flow Jacobian can be selected as proximity indicator for load shed under emergency conditions to avoid risk of voltage instability. The amount of load to be shed is decided so as to maintain a threshold value of indicator and all load bus voltages should be within

limits. A technique for improving static voltage stability by rescheduling reactive power control variables has been described in [8] and the algorithm implemented is based on the sensitivities of minimum Eigen value with respect to reactive power control variables. During large-scale disturbances, the stability margin becomes very low and the last line of defence is load shedding which can be done by using an automatic device that processes the local signals, detects the decreased margin and activates the load shedding. But the main disadvantage of this approach results from the fact that the relations between the voltage level and the stability limit depends on the load power factor. This drawback was overcome in [9] where a criterion directly based on the definition of voltage stability and calculation of the derivative of apparent power against admittance dS/dY has been implemented. A catastrophic recovery situation may result due to the application of a wrong set of information by an operator. So, the challenge in applying an expert system to a power network is to introduce procedures for recognizing the impact of system contingencies and develop strategies for restoring the normal operation in an interactive manner with the system operator.

A new voltage stability index called the equivalent node voltage collapse index, based on equivalent system model has been presented in [10]. The equivalent node voltage collapse index can identify both the weakest node causing system instability and the system voltage collapse point when it is near zero. In [11] the power system line outage analysis and contingency ranking was done based on maximum loading Point. Maximum loading point has been estimated in normal steady state condition and also in different line outage condition. Critical line was identified based on the contingency ranking. Four different types of static voltage stability indices to study voltage collapse have been discussed in [12]. These indices were used to identify weakest bus, line and area in the power network and also to obtain reliable information about closeness of the power system to voltage collapse.

In [13] an expert system had been utilized to enhance the performance of the system by implementing load shedding as one of alternatives in the restoration of a large scale power system. According to [14] when the power system load is very high, and/or there exists a large generation-demand imbalance in the power system areas, the load margin to the saddle node bifurcation may be too low and the power system may come close to voltage collapse point. In such situations the load margin had been improved by implementing LP-based optimization load shedding algorithm. The system frequency is the other parameter used to sense the need for a load shedding during an emergency condition arising due to generating power deficiency which will drop the system frequency and can lead to system collapse.

In [15] the optimal load shedding algorithm based on the concept of the static voltage stability margin and its sensitivity values at the maximum loading point had been implemented over the IEEE 14-bus system and solved using a mathematical (GAMS/CONOPT) and two heuristic (Particle Swarm Optimization and Genetic Algorithm) methods.

In [16] an adaptive scheme for load shedding which uses both frequency and rate of change of frequency measurements to dynamically set the under frequency load shedding relays (ULFS) had been implemented. Also a

technique for coordinating UFLS and the activation of spinning reserves through localized governor control has been proposed. Urban and Rafael [17] analysed the factors that influence the frequency gradient and states that, as long as certain factors are ignored or assumed to be constant the frequency gradient can give misleading information about the active power deficit even though it is useful for actual load shedding procedure. In [18] a mathematical model had been developed which would help the system planner and operator to work out the load shedding operation efficiently.

SFLA and ABC algorithms has been implemented in [19] for minimizing the total amount of real power to be shed in the buses selected based on the sensitivities of the buses with respect to a critical line of the system which is identified by the line voltage stability index. In this paper HS algorithm has been implemented for optimizing the total amount of load to be shed on the selected buses [19]. The proposed method has been tested on IEEE 14- bus and IEEE 25-bus test system. The test results were compared and analysed.

2. Line Voltage Stability Index

Let the line connected between the bus $'k'$ and $'m'$ as shown in Fig. 1.

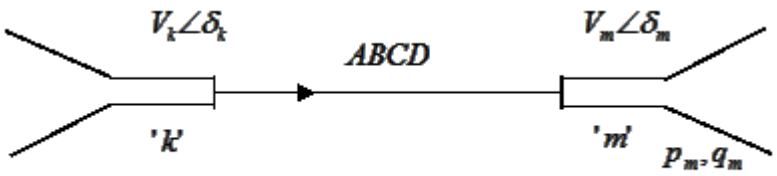

Fig. 1. Single line diagram of the transmission line connecting buses *k* and *m*.

The receiving end real power is

$$P_m = \frac{|V_k|^2}{|B|}\left(\frac{|V_m|}{|V_k|}\cos(\beta-\delta) - \frac{|A||V_m|^2}{|V_k|^2}\cos(\beta-\alpha)\right) \quad (1)$$

where

$$\delta = (\delta_k - \delta_m)$$

Normalizing Eq. (1)

$$p_m = \left(v\cos(\beta-\delta_k+\delta_m) - |A|v^2\cos(\beta-\alpha)\right)$$

$$\text{where, } v = \frac{|V_m|}{|V_k|},\ p_m = \frac{P_m}{P_N} \text{ and } P_N = \frac{|V_k|^2}{B} \quad (2)$$

Similarly the receiving end reactive power is

$$Q_m = \frac{|V_k||V_m|}{|B|}\sin(\beta-\delta) - \frac{|A||V_m|^2}{|B|}\sin(\beta-\alpha) \tag{3}$$

Normalizing Eq. (3)

$$q_m = \left[v\sin(\beta-\delta_k+\delta_m) - Av^2\sin(\beta-\alpha)\right] \tag{4}$$

where $v = \frac{|V_m|}{|V_k|}$, $q_m = \frac{Q_m}{Q_N}$ *and* $Q_N = \frac{|V_k|^2}{B}$

The Jacobian matrix of the transmission line is written as

$$J = \begin{bmatrix} \frac{\partial p_m}{\partial \delta_m} & \frac{\partial p_m}{\partial v} \\ \frac{\partial q_m}{\partial \delta_m} & \frac{\partial q_m}{\partial v} \end{bmatrix} \tag{5}$$

At the collapse point the determinant of Jacobian is zero that is $|J| = 0$

$$\therefore \frac{\partial p_m}{\partial \delta_m}\frac{\partial q_m}{\partial v} - \frac{\partial p_m}{\partial v}\frac{\partial q_m}{\partial \delta_m} = 0 \tag{6}$$

Partial differentiation of Eqs. (2) and (4) with respect to δ_m and v and substitution in Eq. (6) gives

$$\begin{aligned} 2Av\cos(\delta-\alpha) &= 1 \\ Av\cos(\delta-\alpha) &= 0.5 \end{aligned} \tag{7}$$

It is clear that Eq. (7) holds good at the collapse point.

Now the following relation is defined as the Line voltage stability index of i^{th} line as

$$L_i = Av\cos(\delta-\alpha) \tag{8}$$

where A=Transmission line constant

For short transmission line $A = 1$

For medium transmission line $A = \left(1+\frac{zy}{2}\right)$

For long transmission line $A = \cosh\gamma l$ where $\gamma = (\alpha + j\beta)$

$\alpha \Rightarrow$ The phase angle of A constant

It has been established that for a system to be stable, the value of L_i for the lines in a power network must be greater than 0.5. From no load to voltage collapse point, the value of line voltage stability index varies from $A\cos(\alpha)$ (= nearly one) to 0.5. The lines can be ranked based on the magnitudes of this line voltage stability index.

This L index depends on

- A is constant of transmission line

- Ratio of receiving end voltages to sending end voltages.
- Phase angle across the line.

Therefore the loadability of the long transmission line decreases owing to decrease in magnitude of 'A'.

At MLP the line voltage stability index of one of the lines becomes very low as compared to the other lines and this line is considered as critical line. Sensitivities of this critical line with respect to real and reactive power injections are used for the selection of buses for load shed.

The sensitivities are defined as $\frac{\partial L_i}{\partial Q_r} = b_{ir}$; $\frac{\partial L_i}{\partial P_r} = a_{ir}$ where a_{ir}, b_{ir} are sensitivity coefficients of line voltage stability index of the i^{th} line (critical line) with respect to the real and reactive power injection changes at the r^{th} bus respectively. a_{ir}, b_{ir} can be obtained by partial differentiation Eq. (8) with respect to real and reactive power injections.

$$a_{ir} = \frac{A_i}{V_k^2}\left[V_k \frac{\partial V_m}{\partial P_r}\cos(\delta-\alpha) - V_m \frac{\partial V_k}{\partial P_r}\cos(\delta-\alpha)\right] - A_i \frac{V_m}{V_k}\sin(\delta-\alpha)\left(\frac{\partial \delta_k}{\partial P_r} - \frac{\partial \delta_m}{\partial P_r}\right) \tag{9}$$

$$b_{ir} = \frac{A_i}{V_k^2}\left[V_k \frac{\partial V_m}{\partial Q_r}\cos(\delta-\alpha) - V_m \frac{\partial V_k}{\partial Q_r}\cos(\delta-\alpha)\right] - A_i \frac{V_m}{V_k}\sin(\delta-\alpha)\left(\frac{\partial \delta_k}{\partial Q_r} - \frac{\partial \delta_m}{\partial Q_r}\right) \tag{10}$$

In Eqs. (9) and (10) the partial derivatives are directly obtained at the end of N-R load flow solution as elements of inverted matrix of load flow Jacobian [8].Total change in line voltage stability index of critical line may be written using sensitivities a_{ir} and b_{ir} as

$$\Delta L_i = a_{ir}\Delta P_r + b_{ir}\Delta Q_r \tag{11}$$

Assuming constant power factor load Eq. (11) can be written as

$$\Delta L_i = (a_{ir} + \beta_r b_{ir})\Delta P_r \tag{12}$$

where $\beta_r = \tan\phi_r = \frac{\Delta Q_r}{\Delta P_r}$ and ϕ_r is the power factor angle of the r^{th} bus. The buses are selected for load-shed according to the sensitivity of line voltage stability index of critical line with respect to load-shed at the buses.

3. Problem Formulation for Optimal Load Shedding

The objective function is defined as minimization of total real power load to be shed.

$$J = \sum_{i \in NLS} LS_i \tag{13}$$

where *NLS* is set of buses selected for load-shed.

This function is subject to the following constraints

(i) $$0 \le LS_i \le LS_{i\max} \qquad i \ge NLS \tag{14}$$

where LS_i is amount of real power load-shed and LS_{imas} maximum permissible load-shed at i^{th} bus.

Actually the permissible load shed is a fraction of total load at each selected bus. It may be considered the permissible amount of load shed is 90% of the total load at that bus and the remaining 10% of the total load may be required during emergency condition.

(ii) After load shed voltage of all load buses should be within the limit

$$V_{i\min} \le V_i \le V_{i\max} \qquad i = N_{G+1}.....N_B \tag{15}$$

(iii) Stability constraints: All line voltage stability indices should be greater than threshold values.

$$L_i \ge L_{ith} \qquad i = 1, 2,.....N_C \tag{16}$$

4. Harmony Search Algorithm

In recent years for solving complex engineering optimization problems, the modern optimization methods, also called non-traditional optimization methods, have emerged as a powerful and popular method to obtain better solutions. These techniques are versatile in solving multidimensional and complex non-linear equations. In fact, a vast majority of non-traditional optimization techniques are usually heuristic and/or meta heuristic. The harmony search algorithm is a population based meta heuristic optimization algorithm [20]. It is a stochastic random search technique that does not require specific initial value settings of the decision variables and the derivative information for optimization.

The effort of musicians to find the harmony in music is analogous to the search for a best state (i.e., global optimum) in an optimization process. The HS algorithm has several advantages compared to the traditional optimization techniques and has been very successful in solving a wide variety of optimization problems [21, 22]. This algorithm is inspired by the music improvisation process in which the musician seeks for harmony and continues to tune the pitches to obtain a better harmony [23].

In HS algorithm each musician corresponds to a decision variable; pitch range of musical instruments corresponds to a range of values for the decision variables: aesthetics of an audience corresponds to the objective function; musical harmony at a particular time corresponds to a solution vector at certain iteration. Similar to the improvement of musical harmony, a solution vector is also improved iteration by iteration. Such similarities between two processes can be used to develop a new algorithm by learning from each other. Harmony search is just such a successful example for transforming the qualitative improvisation process in to quantitative optimization process with some idealized rules.

From the following improvisation process adopted by a skilled musician, the working of HS algorithm is better understood. During this process, the musician has one of the following choices:

- A playing the famous tune, a familiar melody from his or her memory that characterizes the music piece.
- playing something similar to the known tune from the memorized theme by changing or adjusting pitches of the memorized theme.
- playing random tunes is the another choice of the musician.

The working of HS approach mimics these choices. The design parameters of the HS algorithm are:

- Harmony is the set of the values of all the variables of the objective function. Each harmony is a possible solution vector.
- Harmony memory (*HM*) is the location where harmonies are stored.
- Harmony memory size (*HMS*) is the number of solution vectors in the harmony memory.
- Harmony memory considering rate (*HMCR*) is the probability of selecting a component from the *HM* members
- Pitch adjusting rate (*PAR*) determines the probability of selecting a candidate from the *HM*.

The HS algorithm consists of the following steps

Step 1: Initialization of the optimization problem and algorithm parameters

The problem to be optimized is formulated in the structure of optimization problem, having an objective function and constraints as

$$\begin{aligned} &Minimise\ (or\ Maximise)\ f(\vec{x}) \\ &subject\ to\ x_i \in X_i, \qquad i = 1,2,3....N \end{aligned} \tag{17}$$

where $f(\vec{x})$ is the objective function with $\vec{x}$ as the solution vector composed of decision variables x_i, and X_i is the set of feasible range of values for each decision variable x_i $\left({}_L x_i \le X_i \le {}_U x_i\right)$, where ${}_L x_i$ and ${}_U x_i$ are the respective lower and upper limits for each decision variable. N is the number of decision variables of the problem. The values of the various parameters of HS algorithm like *HMS*, *HMCR*, *PAR* and the maximum number of iterations are also specified in this step.

Step 2: Initialization of the Harmony Memory (*HM*)

The harmony memory is initialized by randomly generating *HMS* number of solution vectors for the formulated optimization problem. Each component of the solution vector in *HM* is initialized using the uniformly distributed random number between the lower and upper bounds of the corresponding decision variable $\left[{}_L x_i, {}_U x_i\right]$, where $1 \le i \le N$. The i^{th} component of the j^{th} solution vector is as follows

$$x_i^j = {}_L x_i + \left({}_U x_i - {}_L x_i\right).rand[0,1] \tag{18}$$

where $j = 1, 2, 3, \ldots\ldots, HMS$ and $rand[0,1]$ is a uniformly generated random number between 0 and 1.

The HM matrix with HMS number of solution vectors is expressed as

$$HM = \begin{bmatrix} x_1^1 & x_2^1 & \cdots & x_{N-1}^1 & x_N^1 \\ x_1^2 & x_2^2 & \cdots & x_{N-1}^2 & x_N^2 \\ \vdots & \vdots & \vdots & \vdots & \vdots \\ x_1^{HMS-1} & x_2^{HMS-1} & \cdots & x_{N-1}^{HMS-1} & x_N^{HMS-1} \\ x_1^{HMS} & x_2^{HMS} & \cdots & x_{N-1}^{HMS} & x_N^{HMS} \end{bmatrix} \tag{19}$$

Step 3: Improvisation of new harmony from the *HM*

HM is improved by generating a new harmony vector

$\vec{x}' = (x_1' \;\; x_2' \;\; x_3' \;\; \cdots \;\; \cdots \;\; \cdots \;\; \cdots \;\; x_N')$.

Each component of the this vector is generated using

$$x_i' \leftarrow \begin{cases} x_i' \in HM(i) & with\ probability\ \ HMCR \\ x_i' \in X_i & with\ probability\ \ (1 - HMCR) \end{cases} \tag{20}$$

where $HM(i)$ is the i^{th} column of the HM. As the *HMCR* is already defined as the probability of selecting a component from the HM members then $(1 - HMCR)$ is the probability of randomly generating a component within the range of values.

After the generation of x_i' from the *HM* it is further mutated (i.e., pitch adjustment) according to *PAR* which determines whether the generated component is to be adjusted or not. The pitch adjustment for a generated x_i' is given as

$$x_i' \leftarrow \begin{cases} x_i' \pm rand[0,1].bw & with\ probability\ PAR \\ x_i' & with\ probability\ (1 - PAR) \end{cases} \tag{21}$$

where bw is the pitch bandwidth.

Step 4: Updating the *HM*

For updating the *HM*, the value of the objective function is calculated using the newly generated harmony vector $\vec{x}_i'$. If this new value is better than the worst harmony in the HM, judged in terms of the objective function value, then the HM is updated by replacing the worst harmony by the new harmony.

The steps 3 and 4 are repeated until the maximum number of iterations is reached. Finally, the best solution is chosen from the final *HM* and it is considered as the optimal solution for the formulated optimization problem. The flow chart of the HS algorithm is shown in Fig. 2 [23].

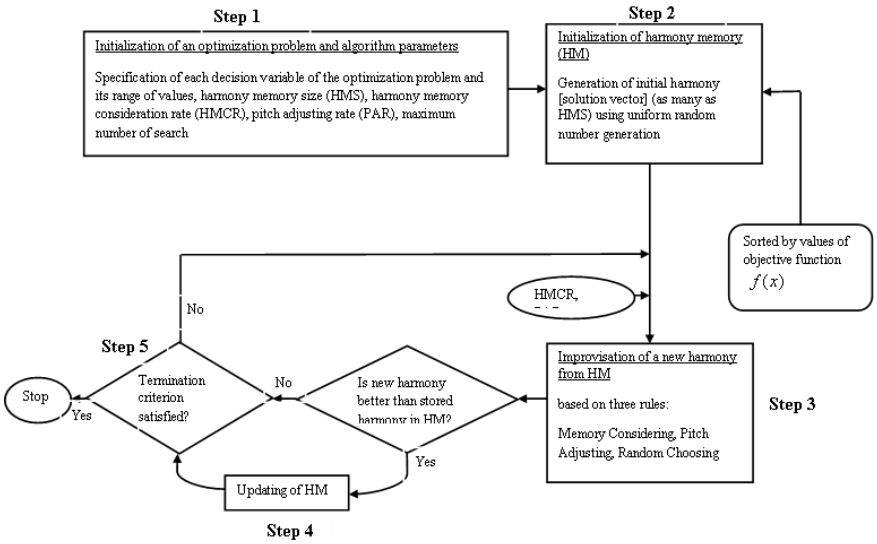

Fig. 2. Flow chart of HS algorithm.

5. Simulation Results and Analysis

The proposed methodology for optimal load shedding has been implemented for the IEEE 14-bus and 25-bus standard test systems. The optimization problem is solved using a music inspired meta heuristic algorithm HS algorithm. The threshold value of all the line voltage stability indices is selected as 0.6. The limits on the load bus voltage are fixed between 0.87 and 1.05 pu. In this paper, the permissible amount of load-shed in each of the selected buses is assumed to be 90% of the total load. The per unit values of bus voltages, line voltage stability index and the static voltage stability margin before and after load shedding are obtained using the proposed algorithms for the test systems considered.

5.1. Case A: IEEE 14-bus test system

This system consists of five synchronous machines, including one synchronous compensator used only for reactive power support and four generators located at buses 1, 2, 6, and 8. In the system, there are 20 branches and 14 buses with 11 loads. The complete data of this test system is taken from [24]. The maximum loading point for this test system is obtained by the continuation power flow (CPF) technique. The base load of the test system is 2.59 pu and 0.735 pu real and reactive powers respectively. The load at the maximum loading point, as obtained by the CPF technique, is 9.4349 pu and 2.6775 pu real and reactive powers respectively. The voltage stability margin before load shedding, in terms of the real and reactive power distance, is 0.11956 up and 0.033935 pu respectively. This margin is inadequate. The line voltage stability index for all the lines is determined at this maximum loading point using Eq. (8). The line number 4 is identified as a critical line whose line voltage stability index is 0.3807 (which is the least).

The sensitivities of the line voltage stability index of the critical line with respect to the load-shed at all the buses are evaluated using Eqs. (9) and (10). Load buses 9, 10, 13 and 14 are found to have the highest sensitivities and these buses are selected for load shedding. Out of these selected buses bus 14 is the one having highest sensitivity and therefore can be considered as the weakest bus for voltage collapse. In [10] a new node voltage stability index based on local voltage phasors was used to identify the weakest buses. Bus 14 was identified as the weakest bus causing system voltage instability by this method. In [11], bus 14 was identified as weakest bus using continuation power flow. Buses 10, 12, 14 were identified as weakest buses based on four different line stability indices presented in [12]. The comparison shows that bus 14 was identified as the weakest bus in this paper and in [10-12].

The proposed HS algorithm is implemented to optimize the total amount of load to be shed in the selected buses. Table 1 shows the optimal load shedding obtained at the selected buses and the magnitude of the total load shed obtained by the proposed method and by the other methods presented in [19]. The amount of load-shed obtained by the proposed HS algorithm is 1.6118 pu whereas the total amount of load shed using shuffled frog leaping algorithm (SFLA) and artificial bee colony algorithm (ABC) presented in [19] are 1.9687 pu and 1.8754 pu respectively. This result shows that the HS algorithm has better search capabilities to find the optimal or near optimal solutions. Figure 3 shows the convergence characteristics of the HS algorithm for IEEE 14-bus system at maximum loading point. The maximum iterations to converge for the proposed approach are 150 iterations.

Table 1. Optimal load shed at selected buses for IEEE 14 - bus system.

Method	Amount of load-shed (pu) at selected bus				
	Bus 9	Bus 10	Bus 13	Bus 14	Total load shed (pu)
SFLA [19]	0.8660	0.2951	0.3558	0.4519	1.9687
ABC [19]	0.7654	0.2951	0.3264	0.4885	1.8754
HSA	0.6102	0.2951	0.3590	0.3475	1.6118

The magnitudes of the voltages of the selected buses obtained before and after load shedding using the proposed method and presented by the methods in [19] is shown in Table 2. From this table it is observed that, before load shedding, the bus voltages of the selected buses are very low at the maximum loading point.

Table 2. Voltage before and after loads at selected buses for IEEE 14-bus system.

Condition	Bus voltage (pu) at selected bus			
	Bus 9	Bus 10	Bus 13	Bus 14
Before load Shedding	0.7077	0.7239	0.8898	0.6814
Afterload shedding using SFLA [19]	0.8739	0.8772	0.9561	0.8700
After load shedding using ABC [19]	0.8706	0.7844	0.9549	0.8708
After load shedding using HSA	0.8822	0.8889	0.9612	0.8749

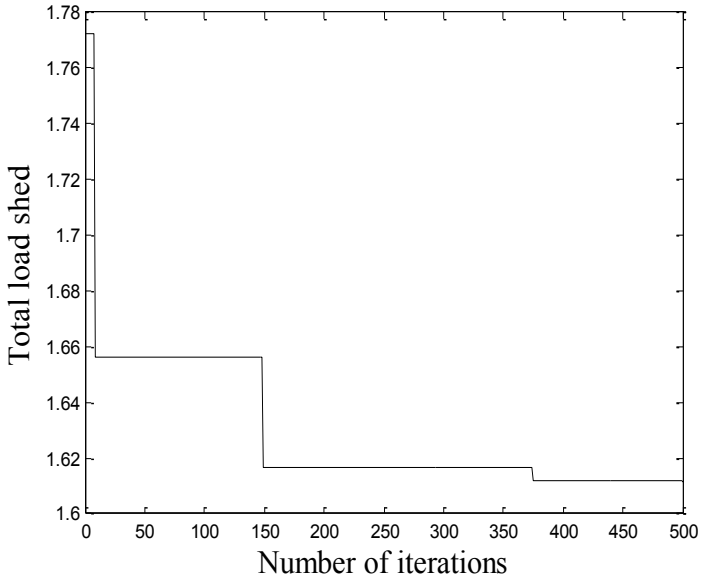

Fig. 3. Convergence characteristics of HS algorithm for IEEE 14 bus system.

The voltage magnitude of the weakest bus (Bus 14) is 0.6814 pu. Whereas in [11] the voltage magnitude of the identified weakest bus (Bus 14) at maximum loading point is 0.6859 pu. It can also be observed that the improvement in all the selected bus voltages after load shedding by the proposed algorithm is better than that of the other methods reported in [19]. This improvement can also be observed in Fig. 4, which shows the bus voltages of all the buses at the maximum loading point obtained by the proposed HS and other algorithms in [19] before and after load shedding.

Table 3 shows the increase in voltage stability margin from the current operating point, after load shedding obtained by the proposed method and by the other methods presented in [19]. The line voltage stability indices for all the lines before and after load-shed obtained by the proposed method and the other methods are shown in Fig. 5. From this figure, it is clear that the line voltage stability indices of all the lines after the load shedding obtained by the proposed method are above the threshold values. The line voltage stability index of the critical line (line 4) after load shedding by the proposed method is 0.9515, which is greater than the threshold value of 0.6 considered. Whereas the line voltage stability index of the critical line obtained after load shedding by SFLA and ABC methods in [19] is 0.9919 and 0.9889 respectively which is slightly greater than that obtained by the proposed method. This is due to the fact that the total amount of load shed by the methods in [19] is greater than that obtained by the proposed HS method. From these analyses of the results obtained by the proposed HS approach for this test system, it is observed that HS algorithm enhances the voltage magnitude of all the selected buses at minimum amount of load shed as compared to that obtained by the other approaches in [19]. It also improves the voltage stability margin of the selected

weak buses after load shedding. These performances of the HS algorithm shows that it is having a good exploitation and exploration characteristics as compared to the other approaches used in [19].

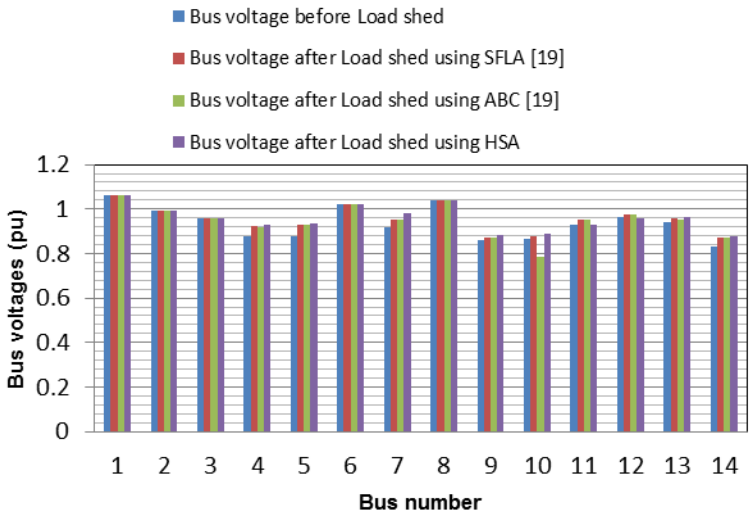

Fig. 4. Bus voltages before and after load shedding using SFLA [19], ABC [19] and HS algorithms for IEEE 14- bus system.

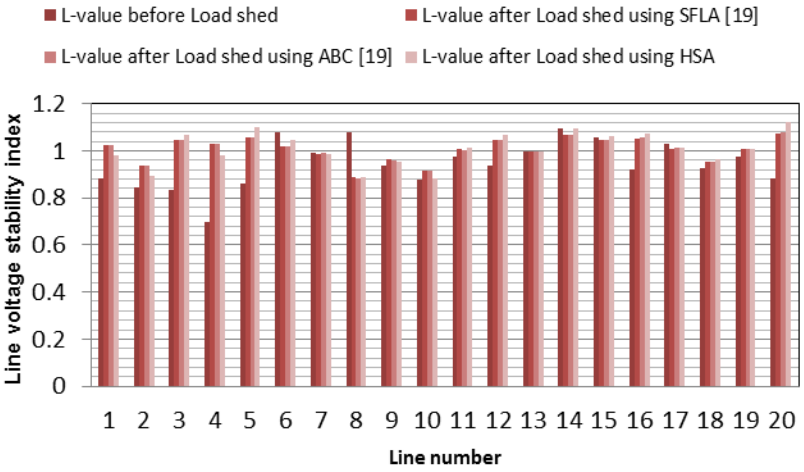

Fig. 5. Line voltage stability index (L-value) before and after load shedding using SFLA [19], ABC [19] and HS algorithms for IEEE 14 bus system.

5.2. Case B: the IEEE 25-bus test system

This system has in all 5 generators, 25 buses and 35 lines. The maximum loading point for this test system is obtained by the CPF technique. The complete data for

this test system is taken from [8]. The base load of the test system is 7.30 pu and 2.28 pu real and reactive powers respectively. The load at maximum loading point, as obtained by the CPF technique, is 16.3155 pu & 5.0958 pu real and reactive powers respectively. The voltage stability margin before load shedding, in terms of real and reactive power distance, is 0.2774 pu and 0.0866 pu respectively. The margin is inadequate. The line voltage stability index for all the lines is determined at this maximum loading point using Eq. (8). The least value of the line voltage stability index is obtained for line number 6. Therefore the line number 6 is identified as critical line. The line voltage stability index of this critical line is 0.5418. This is same as the critical line identified in [7] with line voltage stability index of 0.5054.

Table 3. Voltage stability margin before and after load shed for IEEE 14 - bus system.

Condition	Real (pu)	Reactive
Before load shedding	0.11956	0.03394
After load shedding using SFLA [19]	2.7609	0.99016
After load shedding using ABC [19]	2.6814	0.94974

The sensitivities of the line voltage stability index of the critical line with respect to load-shed at all buses are evaluated using Eqs. (9) and (10). For this system load buses 18, 19, 21, 22, 24 and 25 are found to have the highest sensitivities and these buses are selected for load shedding. The proposed HS algorithm is implemented to optimize the total amount of load to be shed in the selected buses. Table 4 shows the optimal load-shed obtained at these selected buses and the magnitude of total load shed obtained by the proposed method and by the other methods presented in [19]. The amount of load-shed obtained by the proposed method is 1.4107 whereas the amount of load-shed reported in [19] using ABC and SFLA algorithms is 1.775 pu and 1.5597 pu respectively. This result shows that the HS algorithm has better search capabilities to find the optimal or near optimal solutions. Figure 6 shows the convergence characteristics of HS algorithm for the IEEE 25-bus system at the maximum loading point. The maximum iterations to converge for the proposed approach are 90 iterations.

Table 4. Optimal load shed at selected buses for IEEE 25 - bus system.

Method	Amount of load-shed (pu) at selected bus						
	Bus 18	**Bus 19**	**Bus 21**	**Bus 22**	**Bus 24**	**Bus 25**	**Total load Shed (pu)**
SFLA [19]	0.2776	0.2617	0.3228	0.2781	0.2801	0.3572	1.7775
ABC [19]	0.2585	0.2731	0.2650	0.2467	0.2333	0.2831	1.5597
HSA	0.2885	0.1870	0.2011	0.2741	0.2305	0.2295	1.4107

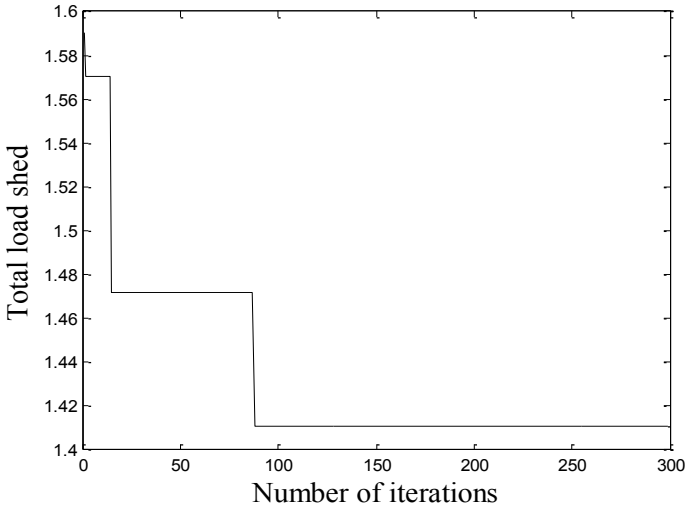

Fig. 6. Convergence characteristics of HS algorithm for IEEE 25- bus system.

Table 5 shows the magnitudes of the voltages of the selected buses obtained before and after load shed by the proposed method is compared with that of the other methods reported in [19]. From the table it is observed that, before load shedding, the bus voltages of the selected buses are very low at the maximum loading point. It can also be observed that there is improvement in the bus voltages of all the selected buses after load shedding by the proposed method. This improvement can also be observed in Fig. 7, which shows the bus voltages of all the buses at the maximum loading point obtained by the proposed HS and other algorithms presented in [19] before and after load shedding.

Table 6 shows the increase in voltage stability margin from the current operating point, after load shedding using HS method and the other methods reported in [19]. Figure 8 shows the line voltage stability indices for all the lines of this system before and after load shedding.

Table 5. Voltage before and after load shed at selected buses for IEEE 25-bus system.

Condition	Bus voltage (pu) at selected bus					
	Bus 18	**Bus 19**	**Bus 21**	**Bus 22**	**Bus 24**	**Bus 25**
Before load shedding	0.8183	0.8732	0.7449	0.6661	0.6314	0.6636
After load shedding using SFLA [19]	0.9434	0.9697	0.9100	0.8929	0.9016	0.9166
After load shedding using ABC [19]	0.9446	0.9695	0.9110	0.8940	0.9034	0.9174
After load shedding using HSA	0.9490	0.9833	0.9362	0.9213	0.9325	0.9407

Table 6. Voltage stability margin before and after load shed for IEEE 25 - bus system.

Voltage stability margin in terms of real and reactive power distance (pu)		
Condition	**Real (pu)**	**Reactive (pu)**
Before load shedding	0.2774	0.0866
After load shedding using SFLA [19]	4.0570	1.4250
After load shedding using ABC [19]	3.7287	1.2882
After load shedding using HSA	3.0741	1.1030

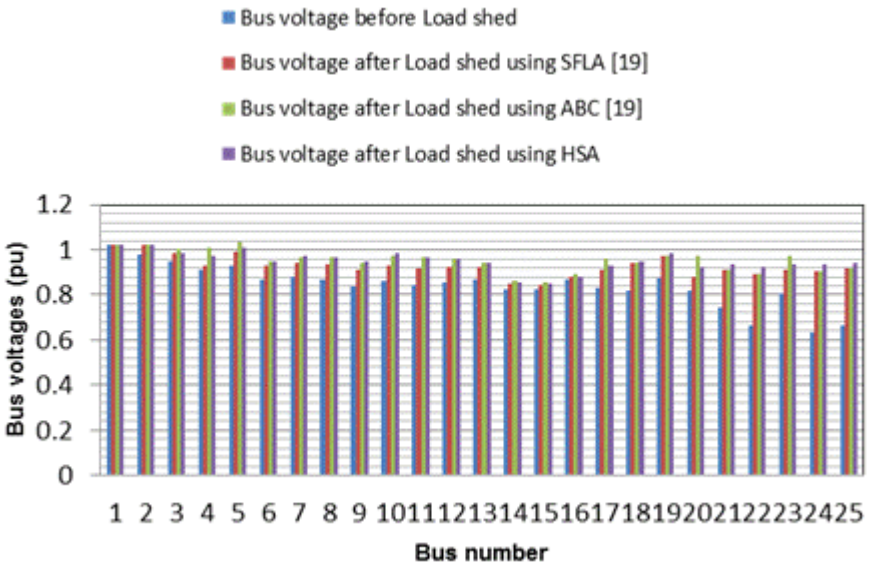

Fig. 7. Bus voltages before and after load shedding using HS algorithm for IEEE 25- bus system.

From Fig. 8 it is clear that the line voltage stability indices of all the lines, after load shedding by proposed method is improved above the threshold values**.** The line voltage stability index of the critical line (line 6) after load shedding by the proposed method is 1.0093 which is greater than the threshold value of 0.6 considered. Whereas the line voltage stability index of the critical line (line 6) after load shedding by the SFLA and ABC methods in [19] was 1.053 pu and 1.0522 pu respectively, which is greater than that obtained by the proposed method. This due to the fact that the total amount of load shed in [19] is greater than that obtained by the proposed HS method.

The result analysis for this test system shows that the proposed HS approach works well in terms of improving the voltage magnitude and voltage stability margin at all the buses including selected buses after shedding the minimum amount of load obtained.

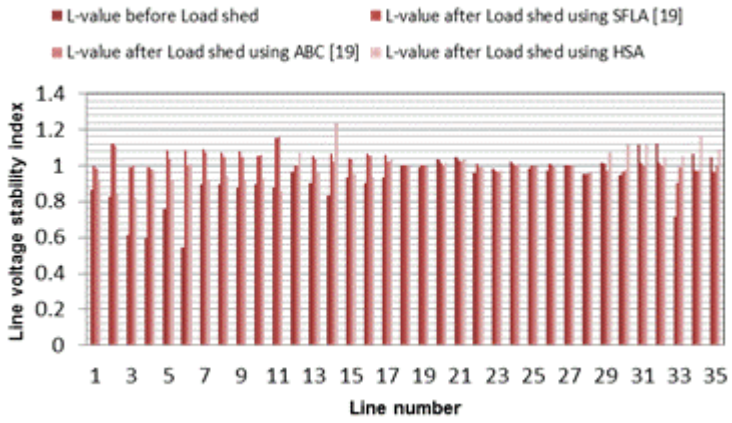

Fig. 8. Line voltage stability index (L-value) before and after load shedding using SFLA [19], ABC [19] and HS algorithms for IEEE 25 bus system.

6. Conclusion

In this paper, the HS algorithm have been implemented for optimal load shedding scheme to obtain adequate voltage stability margin and improvement in the voltage profile of all the load buses. Sensitivities of the line voltage stability index with respect to the load-shed at buses have been used to identify the buses for load shedding. Results have been obtained by implementing the proposed HS algorithm on IEEE 14-bus and IEEE 25-bus test systems. The voltage stability margin which is a measure of the stability of the system has been improved in both the test systems after load shedding. The tabulated results and graphical analysis shows that for the considered optimization problem the proposed HS approach has better performance in terms of convergence and ability to search for a near optimal solution as compared to other approaches presented in [19].

In addition with randomization, pitch adjustment rate (*PAR*) of the proposed algorithm controls the diversification characteristics of the algorithm which is an important factor for the high efficiency of this algorithm. Intensification characteristics of the proposed algorithm are controlled by the harmony memory consideration rate (*HMCR*). The randomization and harmony memory considering rate explores the global search space effectively. Similarly the intensification is enhanced by the controlled pitch adjustment. Such interaction between various components of the algorithm is another important factor for the better performance and success of the HS algorithm over other algorithms.

References

1. Prabha, K. (1994). *Power system stability and control*. McGraw-Hill, ISBN 0-07-035958-X, 1-1199.
2. Arya, L.D.; Shrivastava, M.; and Choube, S.C. (2009). Application of particle swarm optimization and its variants for optimal load shedding. *Iranian journal of Electrical and Computer Engineering*, 8(1), 30-34.

3. Taylor, C.W. (1992). Concept of under voltage load shedding for voltage stability. *IEEE Transaction on Power Delivery*, 7(2), 480-487.
4. Berg, G.J.; and Sharaf, T.A. (1994). System loadability and load shedding. *International Journal of Electric Power System Research*, 28(3), 217-225.
5. Chattopadhyay, D.; and Chakraborti, B.B. (2003). A preventive / corrective model for voltage stability incorporating dynamic load shedding. *International Journal of Electric Power System Research*, 25(5), 363-373.
6. Arya, L.D.; and Shrivastava, M. (2006). Voltage stability evaluation using line voltage stability index. *Journal of Institution of Engineers (India)*, 87(3), 50-54.
7. Arya, L.D.; Choube, S.C.; and Shrivastava, M. (2008). Technique for voltage stability assessment using newly developed line voltage stability index. *International Journal of Energy Conversion and management*, 49(2), 267-275.
8. Arya, L.D.; Sakarvdia, D.K.; and Kothari, D.P. (2005). Corrective rescheduling for static voltage stability control. *International Journal of Electrical power and Energy Systems*, 27(1), 3-12.
9. Wiszniewski, A. (2007). New criteria of voltage stability margin for the purpose of load shedding. *IEEE Transaction on Power Delivery*, 22(3), 1367-1369.
10. Wang, Y.; Wenyuan, Li.; and Jiping, Lu. (2009). A new node voltage stability index based on local voltage phasors. *Electric Power System Research*, 79(1), 265-271.
11. Anbarasan, A.; and Sanavullah, M.Y. (2012). Identification of maximum loading point in power system under critical line outage condition. *European Journal of Scientific Research*, 68(2), 274-282.
12. Jalboub, M.K.; Ihbal, A.M.; Rajamani, H.S.; and Abd-Alhameed R.A. (2011). Determination of static voltage stability margin of the power system prior to voltage collapse. *8th International Multi-Conference on Systems Signals and Devices*, 1-6.
13. Shah, S.; and Shahidehpour, S.M. (1989). A heuristic approach to load shedding scheme. *IEEE Transaction on Power Systems*, 4(4), 1421-1429.
14. Echavarren, F.M.; Lobato, E.; and Rouco, L. (2006). A corrective load shedding scheme to mitigate voltage collapse. *Electrical Power and Energy Systems*, 28(1), 58- 64.
15. Amraee, T.; Mozafari, B.; and Ranjbar, A.M. (2005). An improved model for optimal under voltage load shedding: particle swarm approach. *IEEE Power India Conference*, 723-728.
16. Chuvychinl, V.N.; Gurov, N.S.; Venkata, S.S.; and Brown, R.E. (1996). An adaptive approach to load shedding and spinning reserve control during underfrequency conditions. *IEEE Transactions on Power Systems*, 11(4), 1805-1810.
17. Urban, R.; and Rafael, M. (2011). Analysis of underfrequency load shedding using a frequency gradient. *IEEE Transaction on Power Delivery*, 26(2), 565-575.
18. Hazarika, D.; and Sinha, A.K. (1998). Method for optimal load shedding in case of generation deficiency in a power system. *Electrical Power and Energy Systems,* 20(6), 411-420.

19. Mageshvaran, R.; Jayabarathi, T.; and Ramaprabha, D. (2012). Optimal load shedding based on line voltage stability index using shuffled frog leaping algorithm and artificial bee colony algorithm. *International Review of Electrical Engineering*, 7(6), 6235-6244.
20. Geem, Z.W. (2009). *Harmony search algorithms for structural design optimization*. Springer-Heidelberg, 239.
21. Geem, Z.W. (2010). *Recent advances in harmony search algorithm*. Springer-Verlag, 270.
22. Geem, Z.W.; Kim, J.H.; and Loganathan, G.V. (2001). A new heuristic optimization algorithm: harmony search. *Simulation*, 76(1), 60-68.
23. Aghaie, M.; Nazari, T.; Zolfaghari, A.; Minuchehr, A.; and Shirani, A. (2013). Investigation of PWR core optimization using harmony search algorithms. *Annals of Nuclear Energy*, 57, 1-15.
24. Christie, R.D. (1999). Power system test case archive. University of Washington, Department of Electrical Engineering. Retrieved March 10, 2011, from http://www.ee.washington.edu/research/pstca/index.html.